

BNL-68328
 PRINCETON/HEP/2001-1
 TRI-PP-01-09
 KEK Preprint 2001-26

Search for the rare decay $K^+ \rightarrow \pi^+ \gamma$

S. Adler¹, M. Aoki^{6(a)}, M. Ardebili⁵, M.S. Atiya¹, A.O. Bazarko⁵, P.C. Bergbusch^{6,8},
 E.W. Blackmore⁶, D.A. Bryman^{6,8}, I-H. Chiang¹, M.R. Convery^{5(b)}, M.V. Diwan¹,
 J.S. Frank¹, J.S. Haggerty¹, T. Inagaki³, M.M. Ito^{5(c)}, V. Jain¹, S. Kabe³,
 M. Kazumori^{3(d)}, S.H. Kettell¹, P. Kitching⁷, M. Kobayashi³, T.K. Komatsubara³,
 A. Konaka⁶, Y. Kuno^{3(e)}, M. Kuriki³, T.F. Kycia^{1(f)}, K.K. Li¹, L.S. Littenberg¹,
 J.A. Macdonald⁶, R.A. McPherson^{5(g)}, P.D. Meyers⁵, J. Mildenerberger⁶, M. Miyajima²,
 N. Muramatsu^{3(d)(h)}, T. Nakano⁴, C. Ng¹⁽ⁱ⁾, J. Nishide², T. Numao⁶, A. Otomo^{3(d)},
 J.-M. Poutissou⁶, R. Poutissou⁶, G. Redlinger^{6(j)}, T. Sasaki⁴, T. Sato³, T. Shinkawa^{3(k)},
 F.C. Shoemaker⁵, R. Soluk⁷, J.R. Stone⁵, R.C. Strand¹, S. Sugimoto³, Y. Tamagawa²,
 C. Witzig¹, and Y. Yoshimura³
 (E787 Collaboration)

¹*Brookhaven National Laboratory, Upton, New York 11973*

²*Department of Applied Physics, Fukui University, 3-9-1 Bunkyo, Fukui, Fukui 910-8507, Japan*

³*High Energy Accelerator Research Organization (KEK), Oho, Tsukuba, Ibaraki 305-0801, Japan*

⁴*RCNP, Osaka University, 10-1 Mihogaoka, Ibaraki, Osaka 567-0047, Japan*

⁵*Joseph Henry Laboratories, Princeton University, Princeton, New Jersey 08544*

⁶*TRIUMF, 4004 Wesbrook Mall, Vancouver, British Columbia, Canada, V6T 2A3*

⁷*Centre for Subatomic Research, University of Alberta, Edmonton, Alberta, Canada, T6G 2N5*

⁸*Department of Physics and Astronomy, University of British Columbia, Vancouver, BC,
 Canada, V6T 1Z1*

Abstract

We have performed a search for the angular-momentum forbidden decay $K^+ \rightarrow \pi^+ \gamma$ with the E787 detector at BNL. No events were observed in the π^+ kinematic region around 227 MeV/ c . An upper limit on the branching ratio for the decay is set to be 3.6×10^{-7} at 90% confidence level.

Typeset using REVTeX

I. INTRODUCTION

The decay $K^+ \rightarrow \pi^+ \gamma$ is a $0 \rightarrow 0$ transition with a real photon and is forbidden by angular momentum conservation [1]. This decay is also forbidden on gauge invariance grounds [2]. Historically, the absence of $K^+ \rightarrow \pi^+ \gamma$ relative to the $K^+ \rightarrow \pi^+ \pi^0$ decay ($K_{\pi 2}$) led Dalitz to determine the kaon spin to be zero rather than two or greater [3]. In 1969, a model of strange particles and weak decays predicted this decay at a branching ratio of 2×10^{-4} [4]; the model was later ruled out by an experimental upper limit of 4×10^{-6} at 90% confidence level (C.L.) [5].

No theory of physics beyond the Standard Model, if it is based on point-particle quantum field theory, allows the $K^+ \rightarrow \pi^+ \gamma$ decay. Current interest in the decay mode stems from theoretical speculation that an experimental signature of exotic physics, such as a vacuum expectation value to a new vector field [6], non-local Superstring effects [7], or departures from Lorentz invariance [8], could appear in this decay mode. No specific theoretical prediction or bound on the branching ratio has yet been given.

In previous experiments [5,9] no candidate events were detected. The most recent upper limit of 1.4×10^{-6} at 90% C.L. [9] was established in 1982.

II. DETECTOR

The new search reported here used the E787 detector [10] (see Fig. 1) at the Alternating Gradient Synchrotron (AGS) of Brookhaven National Laboratory (BNL). E787 is a rare kaon-decay experiment studying $K^+ \rightarrow \pi^+ \nu \bar{\nu}$ [11] and related decays [12]. The AGS delivered kaons of about 700 MeV/c to the experiment at a rate of $(4 - 7) \times 10^6$ per 1.6-s spill. The kaon beam line [13] incorporated two stages of electrostatic particle separators which reduced the pion contamination to 25% at the entrance of the detector. Kaons were detected and identified by a Čerenkov counter, multi-wire proportional chambers and an energy-loss counter. After being slowed by a BeO degrader, approximately 25% of the incident kaons stopped in an active target located at the center of the detector. The 12-cm diameter target, which consisted of 0.5-cm square plastic-scintillating fibers, provided initial tracking of the stopping kaon and its decay products.

Particles emanating from kaon decays at rest in the target were measured in a solenoidal spectrometer with a 1.0-T field along the beam axis. The charged decay products passed through a layer of trigger scintillators surrounding the target (I-counter) and a cylindrical drift chamber [14], and lost energy and stopped in a Range Stack (RS) of plastic scintillators. The drift chamber, with a total mass of 3×10^{-2} radiation lengths, provided tracking information from 12 layers of axial anode-wire cells and six layers of thin spiral-strip cathode foils. The RS filled the radial region between 45.1 cm and 89.6 cm and was segmented into 24 azimuthal sectors and 21 radial layers totaling one radiation length. The first RS layer (T-counter), which defined the solid angle acceptance for the π^+ track in the RS, was 0.635-cm thick and 52-cm long; the subsequent RS counters from the second layer (RS2-counter) and beyond were 1.905-cm thick and 182-cm long. Two layers of straw-tube tracking chambers were embedded within the RS. The output pulse shapes of the RS counters were recorded by 500-MHz sampling transient digitizers (TDs) [15], each of which was based on two interleaved 250-MHz flash analog-to-digital converters (ADCs). In addition to providing precise

time and energy information for reconstructing the π^+ track, the TDs provided rejection of muon and electron tracks by detecting the $\pi^+ \rightarrow \mu^+$ decay in the RS stopping counter.

A hermetic calorimeter system, designed primarily to veto photons from $K_{\pi 2}$ and other decays in the $K^+ \rightarrow \pi^+ \nu \bar{\nu}$ study, surrounded the central region. The cylindrical barrel (BL) calorimeter covering about two thirds of the solid angle, and located immediately outside the RS, was used to search for the photon from the $K^+ \rightarrow \pi^+ \gamma$ decay. It consisted of alternating layers of lead (0.1 cm) and plastic scintillator (0.5 cm) sheets and was segmented azimuthally into 48 sectors whose boundaries were tilted so that the inter-sector gaps did not project back to the target. In each sector, four radial groups of 16, 18, 20 and 21 lead-scintillator layers, respectively with increasing radius, totaled 14.3 radiation lengths. About 29% of the shower energy was deposited in the scintillators. The z position (along the beam axis) of the BL hits was measured with time-to-digital converter (TDC) and ADC information from phototubes on both ends of the 190-cm long modules, and was used to determine the polar opening angle between the photon and the π^+ track. The two endcap calorimeters [16] and additional calorimeters for filling minor openings along the beam direction, as well as any active parts of the detector not hit by the π^+ track, were used for vetoing extra particles including photons. The two endcap calorimeters consisted of 143 undoped-CsI crystals, which were read out by 500-MHz TDs based on charged coupled devices [17].

III. TRIGGER

The $K^+ \rightarrow \pi^+ \gamma$ trigger required a kaon decay at rest, a π^+ track in the RS, a shower cluster in the BL and no extra particles in the BL, endcap or RS counters. A kaon was identified in the trigger by a coincidence of hits from the Čerenkov counter, energy-loss counter and target. An online delayed coincidence (> 1.5 ns) of the timing between the incoming kaon (via the Čerenkov counter) and the outgoing pion (via the I-counter) removed contributions from beam pions which were scattered into the detector and from kaons which decayed in flight. A single charged track was required to have a coincidence of the hits from the I-counter and from the T-counter and RS2-counter in the same RS sector. The track was also required to penetrate to at least the sixth RS layer in the sector with a T-RS2 coincidence or in either of the next two clockwise sectors, in order to accept a positively charged particle. Tracks reaching the outer three RS layers (19 – 21) were vetoed to suppress the muons from $K^+ \rightarrow \mu^+ \nu$ and $K^+ \rightarrow \mu^+ \nu \gamma$ decays. Based on the pulse shape information from the TDs on the RS, events with a $\pi^+ \rightarrow \mu^+$ decay in the RS stopping counter were tagged online by a double-pulse algorithm demanding that the RS pulse had a larger area (due to the μ^+) than expected from its height, in order to further reduce muon and electron tracks. By summing the energy of the BL counters in the adjacent two sectors and discriminating it with a threshold of 10 MeV, the number of shower clusters in the BL calorimeter was counted online and was restricted to be one. An event was vetoed if the energy observed in the endcap calorimeter was more than 20 MeV or the energy in the RS sectors outside the region of the π^+ track was more than 10 MeV.

The trigger was pre-scaled by 2450 for taking data simultaneously with the trigger for $K^+ \rightarrow \pi^+ \nu \bar{\nu}$. The total exposure of kaons entering the target available for the $K^+ \rightarrow \pi^+ \gamma$ search was 6.7×10^8 , and a total of 1.6×10^6 events met the trigger requirements. Most of them were due to $K_{\pi 2}$.

IV. OFFLINE ANALYSIS

The signature of $K^+ \rightarrow \pi^+ \gamma$ is a two-body decay of a kaon at rest with a 227-MeV/ c π^+ track in the RS and a 227-MeV photon emitted directly opposite to it and observed as a single BL cluster. It is assumed that energy-momentum is conserved or that its violation due to exotic physics is tiny and undetectable in this decay mode.

The RS energy calibration was done for each end separately, using the energy loss of the muons from the $K^+ \rightarrow \mu^+ \nu$ decay in each counter. Calibration of the BL calorimeter was performed using the energy depositions from cosmic rays, and was verified by reconstructing the energy of the π^0 in $K_{\pi 2}$ decay. The π^+ track in the RS defined the event time reference, and $K_{\pi 2}$ was used to determine the time calibration of the BL calorimeter in the TDCs.

In the offline analysis, the timing, the magnitude (P) and direction of the momentum, the range (equivalent cm of scintillator, R) and the kinetic energy (E) of the π^+ track were reconstructed with the target, drift chamber and RS information. In order to measure the range with positions recorded in the RS tracking chambers, a stopping-layer cut accepted only events whose π^+ track stopped in the layers beyond the inner RS tracking chamber (from 11 to 18) for analysis. The kinematic resolutions (rms) were $\Delta P = 2.6$ MeV/ c , $\Delta R = 1.28$ cm and $\Delta E = 3.8$ MeV. The timing, energy (E_γ) and direction of the photon were determined from reconstruction of the BL hits and the kaon decay vertex position in the target. The energy resolution of the BL calorimeter was $\Delta E_\gamma / E_\gamma = 6\% / \sqrt{E_\gamma}$ (E_γ in GeV). The resolutions of azimuthal and polar opening angles between the photon and the π^+ track, $\phi_{\pi^+ \gamma}$ and $\theta_{\pi^+ \gamma}$, were determined to be $\Delta \phi_{\pi^+ \gamma} = 2.2^\circ$ and $\Delta \theta_{\pi^+ \gamma} = 3.9^\circ$, respectively.

Taking into consideration the limited energy resolution and segmentation of the BL calorimeter, loose fiducial cuts on the energy and direction of the photon in the BL were imposed: $E_\gamma \geq 120$ MeV, $|\phi_{\pi^+ \gamma}| \geq 165^\circ$ and $\theta_{\pi^+ \gamma} \geq 165^\circ$. A coincidence cut (± 2 ns) between the times of the photon and the π^+ track was imposed, and severely reduced the occurrence of photon candidates due to accidental hits.

An offline delayed-coincidence cut (> 2 ns) between the times of the kaon and the pion in the target and analysis cuts on the timing and energy of the hits recorded in the Čerenkov counter, proportional chambers, energy-loss counter and target were imposed to remove events triggered by kaon decays in flight or by multiple beam particles. A double-pulse fit to the pulse shape recorded in the RS stopping counter was made to ensure $\pi^+ \rightarrow \mu^+$ decay, and to remove contamination from $K^+ \rightarrow \mu^+ \nu$, $K^+ \rightarrow \mu^+ \nu \gamma$, $K^+ \rightarrow \mu^+ \pi^0 \nu$ and $K^+ \rightarrow e^+ \pi^0 \nu$ decays, as well as $K_{\pi 2}$ decays whose π^+ decayed in flight in the detector.

The set of events with a fiducial cut on the π^+ momentum ($218 \leq P \leq 234$ MeV/ c) was identified as the “ $\pi\gamma$ sample”, and the signal region¹ was further specified as the subset of the $\pi\gamma$ sample with the fiducial cuts $35.5 \leq R \leq 40.0$ cm and $120 \leq E \leq 135$ MeV.

¹ This signal region is the same as that for the search for $K^+ \rightarrow \pi^+ X^0$ decay in [11], where X^0 is a neutral weakly interacting massless particle [18].

V. BACKGROUND STUDIES

Background sources were studied from the data before examining the signal region. For each background source, we established two independent sets of offline cuts. One set of cuts was inverted to enhance the background collected by the $K^+ \rightarrow \pi^+ \gamma$ trigger, and the rejection of the other set of cuts was evaluated. This technique prevented candidate events from being examined before the background studies were completed. In order to avoid contamination from other background sources, all other cuts were imposed in advance.

The main background source was $K_{\pi 2}$ decay with a branching ratio of 0.2116 [19] and a π^+ track momentum of 205 MeV/c. The higher energy photon (> 125 MeV) from the $\pi^0 \rightarrow \gamma\gamma$ decay in $K_{\pi 2}$ tends to be emitted opposite the π^+ track. $K_{\pi 2}$ background events can survive if the π^+ track is mis-measured to have larger kinematic values and at the same time the lower energy photon from the π^0 (or the electron-positron pair from the $\pi^0 \rightarrow \gamma e^+ e^-$ decay) is undetected.

The set of events whose π^+ momentum and range were consistent with $K_{\pi 2}$ decay ($197.5 \leq P \leq 212.5$ MeV/c and $27.0 \leq R \leq 35.0$ cm) was identified as the “ $\pi\pi^0$ sample”. This sample was collected by the same $K^+ \rightarrow \pi^+ \gamma$ trigger and was independent of the $\pi\gamma$ sample. It was used for evaluating the rejections of the set of cuts other than the π^+ fiducial cuts as well as for normalization of the sensitivity calculation.

A. Photon veto inefficiency

In the offline analysis, photon shower activity was identified in the various subsystems including the BL calorimeter and the RS as hits in the counters in coincidence with the π^+ track within a few ns and with energy above a low threshold (typically ~ 1 MeV). Events with activity not associated with the π^+ and photon candidates were vetoed. In addition, events in which the photon cluster in the BL showed associated activity in the neighboring RS sectors were vetoed by a “RS preshower” cut, which was imposed in advance to both the $\pi\gamma$ sample and the $\pi\pi^0$ sample.

If two photons from a π^0 hit the same or adjacent BL counters, they form a single high-energy BL cluster opposite the π^+ track and can mimic $K^+ \rightarrow \pi^+ \gamma$ decay. In such cases, due to the kinematics of $K_{\pi 2}$ and subsequent $\pi^0 \rightarrow \gamma\gamma$ decays, the two photons must hit the counters at different z positions. The coincidence cut between the times of the photon and the π^+ track, already imposed, reduced the number of events with two photons in the same BL counter because the mean of the arrival times of the scintillation light at each end of the BL counter was significantly earlier than that of a single photon hit. Furthermore, the BL hits in the cluster were examined to determine the maximum discrepancy among the z measurements with TDC and ADC information. Fig. 2 shows the z discrepancy distribution of the BL clusters in the $\pi\pi^0$ sample which survived all other photon veto cuts. An event was vetoed if the discrepancy was more than 75 cm.

To evaluate the rejection of the offline photon veto cuts (except for the RS preshower cut), the subset of the $\pi\pi^0$ sample whose π^+ kinetic energy was consistent with $K_{\pi 2}$ decay ($97 \leq E \leq 117$ MeV) was examined. By imposing the photon veto cuts on this subset, the rejection was measured to be 13.8 as shown in Fig. 3 (a). Then, in the subset of the $\pi\gamma$ sample which failed at least one of the offline photon veto cuts, the kinematic distributions

of $K_{\pi 2}$ background events which survived the π^+ momentum fiducial cut was studied. The π^+ range versus kinetic energy plot of the events is shown in Fig. 3 (b); there are no events in the signal region and 287 events are consistent with $K_{\pi 2}$ decay in range and kinetic energy. This indicates that no mis-measured tracks are in or around the signal region, and a further background reduction by 13.8 is expected by assuming the π^+ fiducial cuts and the photon veto cuts are independent. The background levels in the signal region and in the $K_{\pi 2}$ region were estimated to be < 0.19 events at 90% C.L. and 22.4 ± 1.3 events, respectively ².

If we further added the assumption that the π^+ range and kinetic energy measurements were not correlated, the number of events in the signal region in Fig. 3 (b) was estimated to be < 0.008 events at 90% C.L. and the background in the signal region was estimated to be < 0.0006 events at 90% C.L.

B. Overlapping photon

The above background study could possibly be confounded by $K_{\pi 2}$ events in which the shower of the lower energy photon from the π^0 overlapped some of the counters hit by the π^+ track. The reconstructed kinetic energy of such tracks could be incorrectly measured due to additional energy deposited in the counters by the overlapping photon. A set of dE/dx cuts, which checked the consistency between the measured energy and range in each of the RS counters, was therefore employed to reject this type of background.

To evaluate the rejection of the dE/dx cuts, we selected events in the $\pi\pi^0$ sample whose π^+ kinetic energy was larger than that from $K_{\pi 2}$ decay and was in the signal region for $K^+ \rightarrow \pi^+\gamma$ ($120 \leq E \leq 135$ MeV). By imposing the dE/dx cuts on this subset, the rejection was measured to be 36.3 as shown in in Fig. 4(a). From the subset of the $\pi\gamma$ sample which failed at least one of the dE/dx cuts, the π^+ range versus kinetic energy plot is shown in Fig. 4(b); again no mis-measured tracks are in or around the signal region. The background in the signal region was estimated to be < 0.07 events at 90% C.L. The estimate is limited by statistics.

C. $K^+ \rightarrow \pi^+\gamma\gamma$ decay

For $K^+ \rightarrow \pi^+\gamma\gamma$ decay in the π^+ momentum region greater than 215 MeV/ c , a 90% C.L. upper limit of 5.0×10^{-7} on the branching ratio has been established [20] (assuming a phase-space kinematic distribution). Consequently its contribution to the $K^+ \rightarrow \pi^+\gamma$ search is negligible at the current sensitivity.

VI. RESULT

² Taking into account the tagging efficiency of the inverted photon veto cuts, the numbers of events in the regions in Fig. 3 (b) were divided by the rejection minus 1.

A. Events in the signal region

Fig. 5 shows the π^+ range versus kinetic energy plot of the events which survived all analysis cuts. No events were observed in the signal region. The group of 20 events around $E = 108$ MeV was due to the $K_{\pi 2}$ background and was consistent with the estimate of the photon veto inefficiency.

B. Sensitivity

The single-event sensitivity for $K^+ \rightarrow \pi^+ \gamma$ decay in this search was obtained by normalizing to the number of $K_{\pi 2}$ events in the $\pi\pi^0$ sample collected by the $K^+ \rightarrow \pi^+ \gamma$ trigger. The π^+ track in the RS and the higher energy photon in the BL calorimeter were reconstructed, and the offline analysis cuts of the $K^+ \rightarrow \pi^+ \gamma$ search except for those sensitive to the photons from π^0 (photon veto cuts, dE/dx cuts and target energy cuts) were imposed. The number of events whose π^+ kinetic energy was consistent with $K_{\pi 2}$ decay in the $\pi\pi^0$ sample was 3.62×10^5 .

Acceptance factors were determined from the sample generated by Monte Carlo simulation and from the data samples of $K_{\pi 2}$ decays³, $K^+ \rightarrow \mu^+ \nu$ decays and scattered beam pions, which were accumulated by calibration triggers simultaneous to the collection of signal candidates. Many systematic uncertainties in the measurement of the acceptance factors for $K^+ \rightarrow \pi^+ \gamma$ and $K_{\pi 2}$ canceled by taking a ratio of acceptances of these decay modes⁴. The factors are summarized in Table I.

The acceptance factors of the π^+ reconstruction cuts (including the trigger requirements) and the fiducial cuts (including the kinematic cuts specifying the signal region and the $K_{\pi 2}$ region and the stopping-layer cut) were estimated primarily from Monte Carlo simulation. Losses due to π^+ nuclear interaction and decay-in-flight before stopping in the RS were estimated from Monte Carlo simulations with these effects turned on and off. The π^+ acceptance factors of the online and offline TD cuts (detecting the $\pi^+ \rightarrow \mu^+$ decay in the RS stopping counter) and of the dE/dx cuts were measured from the sample of scattered beam pions which satisfied the fiducial cuts. The acceptance factor of the target energy cuts was measured from the π^+ tracks in the sample of $K_{\pi 2}$ decays tagged by the two photons from the $\pi^0 \rightarrow \gamma\gamma$ decay in the BL calorimeter. The acceptance factors of the online and offline delayed-coincidence cuts and the analysis cuts on the Čerenkov counter, proportional chambers, energy-loss counter and target were measured from the sample of $K^+ \rightarrow \mu^+ \nu$ decays; since these cuts were not related to the kinematic values of π^+ , these factors were assumed to be the same for both the $K^+ \rightarrow \pi^+ \gamma$ and $K_{\pi 2}$ decays.

³ The sample of $K_{\pi 2}$ decays for measuring acceptance factors in this subsection was accumulated by a calibration trigger which removed the requirements on the shower and visible energy in the BL, endcap and RS counters from the $K^+ \rightarrow \pi^+ \gamma$ trigger.

⁴ In fact, many such factors, such as the fraction of kaons entering the target that decayed at rest ~ 0.72 , were identical.

The acceptance factors of the γ reconstruction and fiducial cuts were estimated from Monte Carlo simulation. The acceptance loss of $K_{\pi 2}$ due to the online photon veto cuts was measured from the sample of $K_{\pi 2}$ decays. A part of the shower from the 227-MeV photon in the $K^+ \rightarrow \pi^+ \gamma$ decay could be detected and vetoed by the online and offline photon veto cuts; such acceptance loss of $K^+ \rightarrow \pi^+ \gamma$ should be taken into account in addition to the loss due to the accidental hits in the detector subsystems. Since a data sample of 227-MeV photons from kaon decays at rest was not available, the acceptance factor was estimated from studies which compared the performance of the photon veto cuts on the photons in Monte Carlo simulation and in the sample of $K_{\pi 2}$ decays. The accidental loss was measured from the sample of $K^+ \rightarrow \mu^+ \nu$ decays. Acceptance losses due to the cuts on the BL hits in the cluster (the coincidence between the times of the photon and the π^+ track and the maximum discrepancy among the z measurements) were confirmed to be negligible from the photons in the sample of $K_{\pi 2}$ decays.

With the total acceptances for $K^+ \rightarrow \pi^+ \gamma$ (0.0143) and for $K^+ \rightarrow \pi^+ \pi^0$ (0.00357) in Table I, the number of surviving $K_{\pi 2}$ events (3.62×10^5) and the $K_{\pi 2}$ branching ratio (0.2116), the single-event sensitivity for $K^+ \rightarrow \pi^+ \gamma$ was $(1.46 \pm 0.09) \times 10^{-7}$, which is four times better than the sensitivity achieved in [9]. The main source of the error (6%) was due to the systematic uncertainty in the acceptance loss of the 227-MeV photon from $K^+ \rightarrow \pi^+ \gamma$ due to the online and offline photon veto cuts.

In order to verify that the sensitivity for $K^+ \rightarrow \pi^+ \gamma$ obtained from the ratio to $K_{\pi 2}$ decay was correct, an absolute branching ratio for $K_{\pi 2}$ in the $\pi\pi^0$ sample relative to the sample of $K^+ \rightarrow \mu^+ \nu$ decays was measured and the result deviated by +6% from the known $K_{\pi 2}$ branching ratio. The shift is assigned to be an additional systematic uncertainty in the acceptance of the π^+ track, most probably due to the uncertainty in π^+ nuclear interaction. The total estimated systematic uncertainty in this search is therefore 8.5%.

VII. CONCLUSION

Since no events were observed in the signal region, in the absence of background and taking 2.44 events instead of zero according to the unified approach [19,21], we set a 90% C.L. upper limit 3.6×10^{-7} on the branching ratio for $K^+ \rightarrow \pi^+ \gamma$ decay as a test of angular momentum conservation in particle physics.

The current search is statistically limited, and there are good prospects to improve the sensitivity further. A new experiment E949 [22], which will continue the study of the $K^+ \rightarrow \pi^+ \nu \bar{\nu}$ decay at BNL, can yield further gains by virtue of a larger kaon exposure, trigger optimization and improved photon detection capability.

ACKNOWLEDGMENTS

We gratefully acknowledge the dedicated effort of the technical staff supporting this experiment and of the Brookhaven Collider-Accelerator Department. This research was supported in part by the U.S. Department of Energy under Contracts No. DE-AC02-98CH10886, W-7405-ENG-36, and grant DE-FG02-91ER40671, by the Ministry of Education, Culture, Sports, Science and Technology of Japan through the Japan-U.S. Cooperative

Research Program in High Energy Physics and under the Grant-in-Aids for Scientific Research, for Encouragement of Young Scientists and for JSPS Fellows, and by the Natural Sciences and Engineering Research Council and the National Research Council of Canada.

REFERENCES

- (a) Now at KEK.
 - (b) Now at SLAC, Menlo Park, California 94025.
 - (c) Now at Thomas Jefferson National Accelerator Facility, Newport News, Virginia 23606.
 - (d) Also at Graduate School of Science, The University of Tokyo, Tokyo 113-0033, Japan.
 - (e) Now at Department of Physics, Osaka University, Osaka 560-0043, Japan.
 - (f) Deceased.
 - (g) Now at Department of Physics and Astronomy, University of Victoria, Victoria, BC, Canada, V8W 3P6.
 - (h) Now at Japan Atomic Energy Research Institute, Sayo, Hyogo 679-5198, Japan.
 - (i) Also at Department of Physics and Astronomy, State University of New York at Stony Brook, Stony Brook, NY 11794-3800.
 - (j) Now at BNL.
 - (k) Now at the National Defense Academy of Japan, Yokosuka, Kanagawa 239-8686, Japan.
- [1] E.g., K. Nishijima, *Fundamental Particles* (W. A. Benjamin, INC., New York, 1963), Sec. 2.12; J.J. Sakurai, *Invariant Principles and Elementary particles* (Princeton University Press, Princeton, New Jersey, 1964), Sec. 2.4.
 - [2] S. Ôneda, S. Sasaki and S. Ozaki, Prog. Theor. Phys. **5**, 165 (1950); H. Fukuda, S. Hayakawa and Y. Miyamoto, *ibid.*, **5**, 352 (1950).
 - [3] R.H. Dalitz, Phys. Rev. **99**, 915 (1955); Proc. Phys. Soc. A **69**, 527 (1956).
 - [4] F. Selleri, Nuovo Cim. A **57**, 678 (1968); *ibid.* **60**, 291 (1969).
 - [5] J.H. Klems *et al.*, Phys. Rev. Lett. **25**, 473 (1970); Phys. Rev. D **4**, 66 (1971).
 - [6] G.L. Kane, in the Proceedings of the 9th European Symposium on Proton-Antiproton Interactions and Fundamental Symmetries, Mainz, F.R.Germany, edited by K. Kleinknecht and E. Klempt, Nucl. Phys. B(Proc.Suppl.) **8**, 469 (1989).
 - [7] G.L. Kane, Phys. Today **50-2**, 40 (1997).
 - [8] S. Coleman and S.L. Glashow, Phys. Rev. D **59**, 116008 (1999).
 - [9] Y. Asano *et al.*, Phys. Lett. B **113**, 195 (1982).
 - [10] M.S. Atiya *et al.*, Nucl. Instrum. Methods Phys. Res. A **321**, 129 (1992).
 - [11] S. Adler *et al.*, Phys. Rev. Lett. **79**, 2204 (1997); S. Adler *et al.*, *ibid.* **84**, 3768 (2000).
 - [12] S. Adler *et al.*, Phys. Rev. Lett. **85**, 2256 (2000); S. Adler *et al.*, *ibid.* **85**, 4856 (2000); S. Adler *et al.*, Phys. Rev. D **63**, 032004 (2001).
 - [13] J. Doornbos *et al.*, Nucl. Instrum. Methods Phys. Res. A **444**, 546 (2000).
 - [14] E.W. Blackmore *et al.*, Nucl. Instrum. Methods Phys. Res. A **404**, 295 (1998).
 - [15] M.S. Atiya *et al.*, Nucl. Instrum. Methods Phys. Res. A **279**, 180 (1989).
 - [16] I-H. Chiang *et al.*, IEEE Trans. Nucl. Sci. **NS-42**, 394 (1995); T.K. Komatsubara *et al.*, Nucl. Instrum. Methods Phys. Res. A **404**, 315 (1998).
 - [17] D.A. Bryman *et al.*, Nucl. Instr. Methods Phys. Res. A **396**, 394 (1997).
 - [18] F. Wilczek, Phys. Rev. Lett. **49**, 1549 (1982).
 - [19] Particle Data Group, D.E. Groom *et al.*, Eur. Phys. J. C **15**, 1 (2000).
 - [20] P. Kitching *et al.*, Phys. Rev. Lett. **79**, 4079 (1997).
 - [21] G.J. Feldman and R.D. Cousins, Phys. Rev. D **57**, 3873 (1998).
 - [22] B. Bassalleck *et al.*, E949 Proposal, BNL-67247, TRI-PP-00-06, 1999. The information on E949 is available through <http://www.phy.bnl.gov/e949/> .

TABLES

Acceptance Factors	$\pi^+\gamma$	$\pi^+\pi^0$	samples
π^+ reconstruction cuts	0.399	0.400	MC, $K_{\mu 2}$
π^+ fiducial cuts	0.830	0.694	MC
π^+ nuclear interaction and decay-in-flight	0.477	0.586	MC
Transient digitizer ($\pi^+ \rightarrow \mu^+$) cuts	0.553	0.592	π_{scat}
dE/dx cuts	0.878	ni(*)	π_{scat}
Target energy cuts	0.924	ni(*)	$K_{\pi 2}$
Other cuts on beam and target	0.606	0.606	$K_{\mu 2}$
γ reconstruction and fiducial cuts	0.693	0.232	MC
Online photon veto cuts to $\pi^+\pi^0$	ni(*)	0.264	$K_{\pi 2}$
Online and offline photon veto cuts to the photon from $\pi^+\gamma$	0.482	ni(*)	MC, $K_{\pi 2}$, $K_{\mu 2}$
Total acceptance	0.0143	0.00357	

TABLE I. Acceptance factors for $K^+ \rightarrow \pi^+\gamma$ and $K^+ \rightarrow \pi^+\pi^0$, and the samples used to determine them. “MC”, “ $K_{\pi 2}$ ”, “ $K_{\mu 2}$ ” and “ π_{scat} ” mean the sample generated by Monte Carlo simulation and the data samples of $K^+ \rightarrow \pi^+\pi^0$ decays, $K^+ \rightarrow \mu^+\nu$ decays and scattered beam pions accumulated by calibration triggers, respectively. The dE/dx cuts, target energy cuts and offline photon veto cuts are not imposed on $K^+ \rightarrow \pi^+\pi^0$. (*) not imposed.

FIGURES

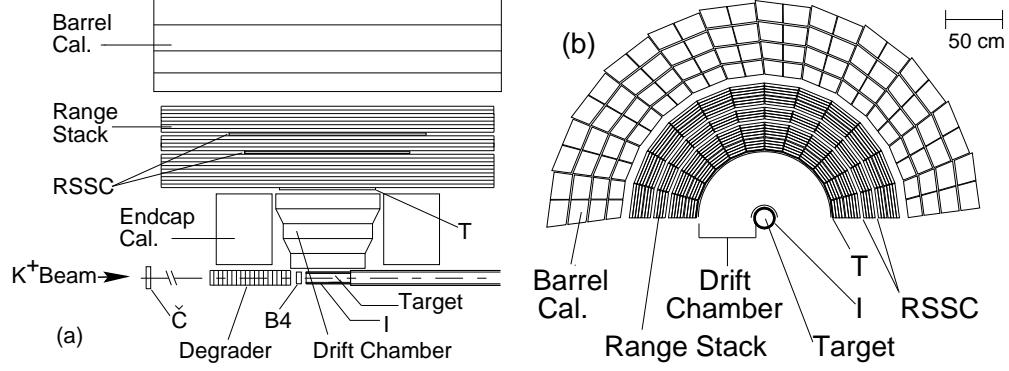


FIG. 1. Schematic side-view (a) and end-view (b) showing the upper half of the E787 detector. Č: Čerenkov counter; B4: energy-loss counter; I and T: trigger scintillators (I-counter and T-counter); RSSC: range-stack straw-tube tracking chambers.

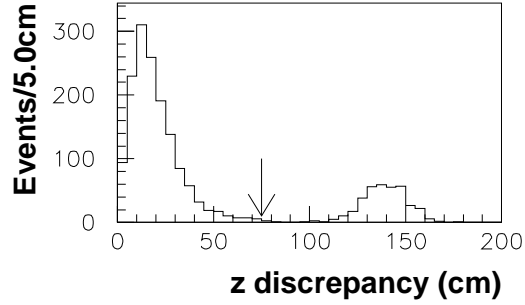


FIG. 2. z discrepancy distribution of the BL clusters in the $\pi\pi^0$ sample with all other photon veto cuts imposed. The arrow indicates the cut position at 75 cm.

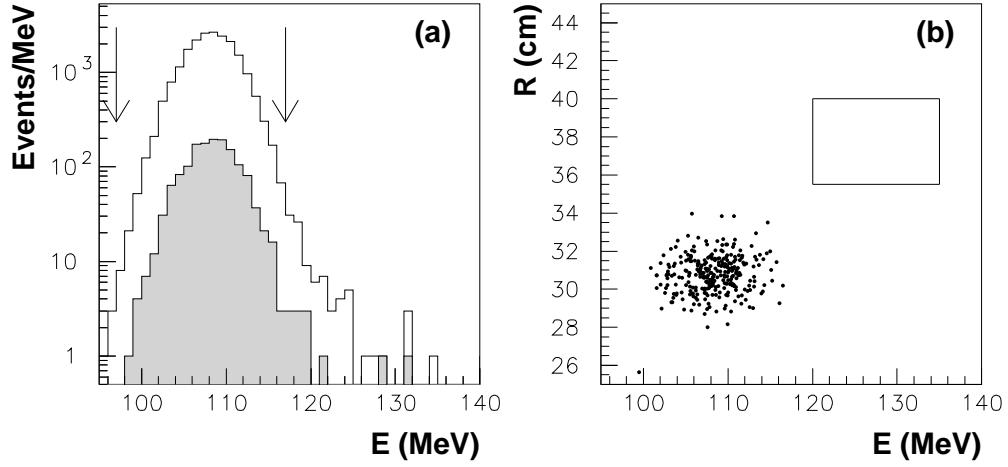


FIG. 3. (a) Kinetic energy distribution of the $\pi\pi^0$ sample. The unhatched and hatched histograms represent the distributions before and after the photon veto cuts are imposed, respectively. The region between the arrows indicates the $K\pi_2$ region. (b) Range versus kinetic energy plot of the events in the subset of the $\pi\gamma$ sample tagged by the inverted photon veto cuts. The box indicates the $K^+ \rightarrow \pi^+\gamma$ signal region.

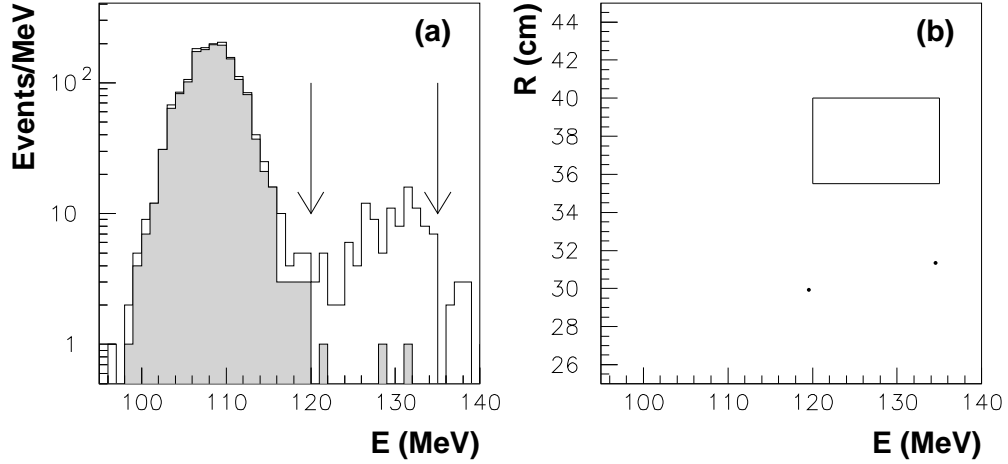


FIG. 4. (a) Kinetic energy distribution of the $\pi\pi^0$ sample. The unhatched and hatched histograms represent the distributions before and after the dE/dx cuts are imposed, respectively. The region between the arrows indicates the signal region for $K^+ \rightarrow \pi^+\gamma$. (b) Range versus kinetic energy plot of the events in the subset of the $\pi\gamma$ sample tagged by the inverted dE/dx cuts. The box indicates the $K^+ \rightarrow \pi^+\gamma$ signal region.

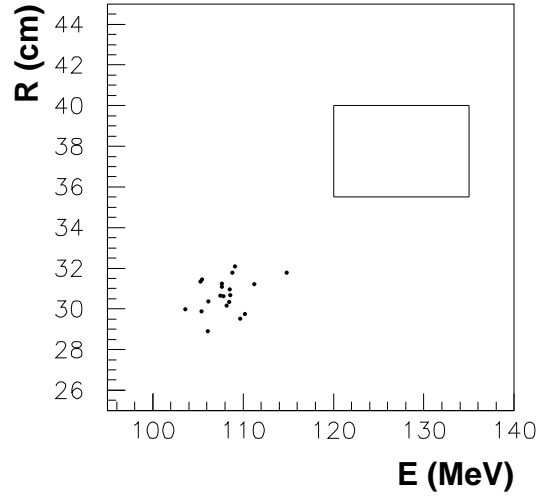


FIG. 5. Range versus kinetic energy plot of the events with all analysis cuts imposed. The box indicates the signal region for $K^+ \rightarrow \pi^+ \gamma$.